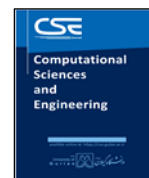




University of Guilan

journal homepage: <https://cse.guilan.ac.ir/>

## Bending and Vibration Analysis of The Third-Order Rectangular Nanoplates Using the Modified Couples Stress Theory

Majid Eskandari Shahraki <sup>a,\*</sup>, Mahmoud Shariati <sup>a</sup>, Naser Asiaban <sup>a</sup>, Ali Davar <sup>b</sup>, Jafar Eskandari Jam <sup>b</sup>, Mohsen Heydari Beni <sup>b</sup>

<sup>a</sup> Faculty of Engineering, Ferdowsi University of Mashhad, Mashhad, Iran.

<sup>d</sup> Faculty of Materials and Manufacturing Technologies, Malek Ashtar University of Technology, Tehran.

### ARTICLE INFO

#### Article history:

Received 24 May 2022

Received in revised form 21 June 2022

Accepted 22 June 2022

Available online 22 June 2022

#### Keywords:

Modified couple stress theory

Third-order Nanoplates

Bending

Vibration

### ABSTRACT

In this paper a third-order rectangular nanoplate model is developed for the bending and vibration analysis of a graphene nanoplate based on a modified couple stress theory. The bending rates and dimensionless bending values under uniform surface traction and sinusoidal load, and the frequencies of the nanoplate are all obtained for various plate's dimensional ratios and material length scale to thickness ratios. The governing equations are numerically solved. The effect of material length scale, length, width and thickness of the nanoplate on the bending and vibration ratios are investigated and the results are presented and discussed in details.

## 1. Introduction

Study of small-scale materials has been the focus of lots of research. It is pointed out that in order to study materials in small scales, experimental approaches give the most reliable results but due the difficulties in running such experiments in small scales these approaches are mostly used as a validation tool for other simpler methods. Atomic simulation is another method to cope with this matter but it is only used for the problems with small deformations because it is extremely cost and time consuming.

In the search to find a better method to model nanostructure materials, researches proposed another method. This method uses continuum mechanics to model small scale structures such as nano materials. There are various size-dependent continuum theories that take into account the effect of the size parameter. All of these theories are the developed notion of classical field theories which include size effects.

Daikh et al, [1] studied A novel nonlocal strain gradient Quasi-3D bending analysis of sigmoid functionally graded sandwich nanoplates. They investigated the effect of the elastic foundation

\* Corresponding author, Email: [majid.eskandari@mail.um.ac.ir](mailto:majid.eskandari@mail.um.ac.ir)

models, sigmoidal distribution index constant, configuration of sandwich plate, material and length nanoscales, boundary conditions on the static deflection.

Yang et al, [2] studied the axisymmetric bending and vibration of circular nanoplates with surface tractions. They investigated the effect of the material's surface properties on the deflection and natural frequencies.

Shafiei et al, [3] employed the modified couple-stress theory to study stability and vibration of single and multi-layered graphene sheets. The effects of different parameters such as loading schemes, nanoplate dimensions and boundary conditions were investigated.

Thanh et al, [4] studied the size-dependent thermal bending and buckling responses of composite laminate microplate based on new modified couple stress theory and isogeometric analysis. The influences of fiber orientation, thickness ratio, boundary conditions and the variation in material length scale parameter were also investigated.

In this paper, size-dependent nanoplate model is developed to account for the size effect. Hamilton principle is used to derive the equations of motion based on the mentioned theories (i.e. modified couple stress and third order shear deformation theories). In order to investigate the effects of material length scale parameter on deflection and frequency, analytical solution is obtained for a simply supported plate and results are discussed.

## 2. Modified couple stress theory

The modified couple stress model was proposed by Yang et al. [5] after developing the theory proposed by Toppin [6], Mindlin and Thursten [7], Quidter [8] and Mindlin [9] in 1964. The advantage of Yang's model is that instead of two parameters, it only needs one material length scale parameter for projection of the size effect. In this theory the strain energy density in the three-dimensional vertical coordinates for a body bounded by the volume  $V$  and the area  $\Omega$  [10], is expressed as the follows:

$$U = \frac{1}{2} \int_V (\sigma_{ij} \varepsilon_{ij} + m_{ij} \chi_{ij}) dV \quad i, j = 1, 2, 3 \quad (1)$$

where:

$$\varepsilon_{ij} = \frac{1}{2} (u_{i,j} + u_{j,i}) \quad (2)$$

$$\chi_{ij} = \frac{1}{2} (\theta_{i,j} + \theta_{j,i}) \quad (3)$$

$\chi_{ij}$  and  $\varepsilon_{ij}$  are the symmetric part of the curvature and strain tensors, respectively, and also,  $\theta_i$  and  $u_i$  are the displacement vector and the rotational vector, respectively.

$$\theta = \frac{1}{2} \text{Curl } \mathbf{u} \quad (4)$$

$\sigma_{ij}$  and  $m_{ij}$  the stress tensor and deviatoric part of the couple stress tensor, respectively, are defined as:

$$\sigma_{ij} = \lambda \varepsilon_{kk} \delta_{ij} + 2\mu \varepsilon_{ij} \tag{5}$$

$$m_{ij} = 2\mu l^2 \chi_{ij} \tag{6}$$

Where  $\lambda$  and  $\mu$  lame constants,  $\delta_{ij}$  is the Kronecker delta and  $l$  is the material length scale parameter. From Equation (3) and (6) it can be seen that  $\chi_{ij}$  and  $m_{ij}$  are symmetric.

### 3. Third-order plate model

The displacement equations for the third-order plate are defined as following:

$$u_1(x, y, z, t) = z \varphi_x(x, y, t) - \frac{4}{3} \left(\frac{1}{h}\right)^2 z^3 \left(\frac{\partial w(x,y,t)}{\partial x} + \varphi_x(x, y, t)\right) \tag{7}$$

$$u_2(x, y, z, t) = z \varphi_y(x, y, t) - \frac{4}{3} \left(\frac{1}{h}\right)^2 z^3 \left(\frac{\partial w(x,y,t)}{\partial y} + \varphi_y(x, y, t)\right)$$

$$u_3(x, y, z, t) = w(x, y, t)$$

Where  $\varphi_x$  and  $\varphi_y$  are the rotations of the normal vector around the  $x$  and  $y$  axis respectively, and  $w$  is the midpoint displacement of the plate in the  $z$ -axis direction.

In Figure 1 an isotropic rectangular nanoplate with length  $a$ , width  $b$  and thickness  $h$  is shown.

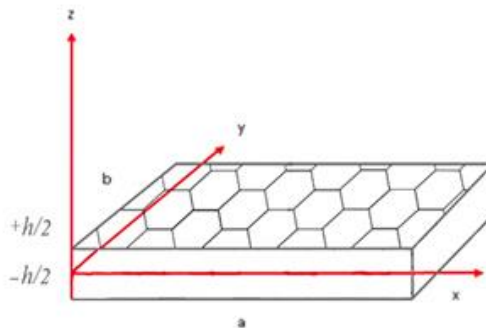


Figure. 1. A schematic of the nanoplate and axes

The strain and stress tensors, the symmetric part of the curvature tensor, and the rotational vector for the  $n$ th-order plate are given in the appendix.

The variation of strain energy is expressed as follows:

$$\delta U = \int_V \sigma_{xx} \delta \varepsilon_{xx} + \sigma_{yy} \delta \varepsilon_{yy} + 2\sigma_{xy} \delta \varepsilon_{xy} + 2\sigma_{xz} \delta \varepsilon_{xz} + 2\sigma_{yz} \delta \varepsilon_{yz} + m_{xx} \delta \chi_{xx} + m_{yy} \delta \chi_{yy} + m_{zz} \delta \chi_{zz} + 2m_{xy} \delta \chi_{xy} + 2m_{xz} \delta \chi_{xz} + 2m_{yz} \delta \chi_{yz} dV$$

To simplify, the coefficients name of the variables can be denoted from  $E_1$  to  $E_{15}$  according to Equation (9) and they are obtained separately. ( $E_1 - E_{15}$  are given in the appendix)

$$\begin{aligned} \delta U = & \int_V (E_1 \delta w_{,xx} + E_2 \delta w_{,yy} + E_3 \delta w_{,xy} + E_4 \delta w_{,x} \\ & + E_5 \delta w_{,y} + E_6 \delta \varphi_{x,yy} + E_7 \delta \varphi_{y,xx} + E_8 \delta \varphi_{y,xy} + E_9 \delta \varphi_{x,yx} \\ & + E_{15} \delta \varphi_y) dV + E_{10} \delta \varphi_{x,x} + E_{11} \delta \varphi_{y,y} + E_{12} \delta \varphi_{x,y} + E_{13} \delta \varphi_{y,x} + E_{14} \delta \varphi_x \end{aligned}$$

#### 4. Virtual work of the external forces [11]

If the middle-plane and the middle-perimeter of the plate are shown as  $\Omega$  and  $\Gamma$  respectively, the virtual work of the external forces can be categorized as, the virtual work done by the body forces applied on the volume  $V = \Omega \times (-h/2, h/2)$ , The virtual work done by the surface tractions at the upper and lower surfaces ( $\Omega$ ) and finally the virtual work of the shear tractions on the lateral surfaces,  $S = \Gamma \times (-h/2, h/2)$ . Considering the body forces ( $f_x, f_y, f_z$ ), the body couples ( $c_x, c_y, c_z$ ), the forces acting on the  $\Omega$  plane ( $q_x, q_y, q_z$ ), the Cauchy's tractions ( $t_x, t_y, t_z$ ) and the surface couples ( $S_x, S_y, S_z$ ) the Variations of the virtual work is obtained as follows:

$$\delta w = - \left[ \int_{\Omega} (f_x \delta u + f_y \delta v + f_z \delta w + q_x \delta u + q_y \delta v + q_z \delta w + c_x \delta \theta_x + c_y \delta \theta_y + c_z \delta \theta_z) dx dy + \int_{\Gamma} (t_x \delta u + t_y \delta v + t_z \delta w + s_x \delta \theta_x + s_y \delta \theta_y + s_z \delta \theta_z) d\Gamma \right] \quad (10)$$

Given that in this study only the external force  $q_z$  is applied, Eq. (10) becomes:

$$\delta w = \int_0^a \int_0^b q(x,y) \delta w(x,y) dx dy \quad (11)$$

The variation of kinetic energy is as follows:

$$\delta T = \int_A \int_{-\frac{h}{2}}^{\frac{h}{2}} \rho (\dot{u}_1 \delta \dot{u}_1 + \dot{u}_2 \delta \dot{u}_2 + \dot{u}_3 \delta \dot{u}_3) dA dz \quad (12)$$

Where  $\rho$  is the density. Also using the Hamilton's principle [12], it can be said:

$$\int_0^T (\delta T - (\delta U - \delta w)) dt = 0 \quad (13)$$

Where  $T$  is kinetic energy,  $U$  is the strain energy, and  $W$  is the external force work.

#### 5. Final governing equations

Using Hamilton's principle Eq. (13), the main equations are obtained: ( $C_1 - C_{12}$  &  $D_1 - D_{13}$  are given in the appendix)

$$\left[ \int_{-h/2}^{h/2} \left( \frac{\partial^2 E_1}{\partial x^2} - \frac{\partial E_4}{\partial x} + \frac{\partial^2 E_2}{\partial y^2} + \frac{\partial^2 E_3}{\partial x \partial y} - \frac{\partial E_5}{\partial y} \right) dz \right] = q(x,y) + \rho I_0 w_{,tt} - C_6^2 \rho I_6 \left( \frac{\partial^2 w}{\partial x^2} + \frac{\partial^2 w}{\partial y^2} \right)_{,tt} + C_6 \rho J_4 \left( \frac{\partial \varphi_x}{\partial x} + \frac{\partial \varphi_y}{\partial y} \right)_{,tt} \quad (14)$$

$$\int_{-h/2}^{h/2} \left( \frac{\partial^2 E_6}{\partial y^2} + \frac{\partial^2 E_9}{\partial x \partial y} - \frac{\partial E_{12}}{\partial y} - \frac{\partial E_{10}}{\partial x} + F_{14} \right) dz = \rho K_2 \varphi_{x,tt} - C_6 \rho J_4 \left( \frac{\partial w}{\partial x} \right)_{,tt} \quad (15)$$

$$\int_{-h/2}^{h/2} \left( \frac{\partial^2 E_7}{\partial x^2} - \frac{\partial E_{13}}{\partial x} + \frac{\partial^2 E_8}{\partial x \partial y} - \frac{\partial E_{11}}{\partial y} + E_{15} \right) dz = \rho K_2 \varphi_{y,tt} - C_6 \rho J_4 \left( \frac{\partial w}{\partial y} \right)_{,tt} \tag{16}$$

coefficients of  $J_4$  and  $K_2$  are obtained as the following:

$$J_4 = I_4 - C_6 I_6 \tag{17}$$

$$K_2 = I_2 - 2C_6 I_4 - C_6^2 I_6 \tag{18}$$

$$I_i = \int_{-\frac{h}{2}}^{\frac{h}{2}} Z^i dz \quad (i = 0, 1, 2, n - 1, n, n + 1, 2n - 4, 2n - 2, 2n) \tag{19}$$

### 6. Third-order plate equations in the general state

The general equations of the third-order plate will be obtained as following:

$$D_1 \frac{\partial^4 w}{\partial x^2 \partial y^2} + D_2 \frac{\partial^4 w}{\partial x^4} + D_2 \frac{\partial^4 w}{\partial y^4} + D_3 \frac{\partial^2 w}{\partial x^2} + D_3 \frac{\partial^2 w}{\partial y^2} + D_4 \frac{\partial^3 \varphi_x}{\partial x^3} + D_4 \frac{\partial^3 \varphi_x}{\partial x \partial y^2} + D_4 \frac{\partial^3 \varphi_y}{\partial y \partial x^2} + D_3 \frac{\partial \varphi_x}{\partial x} + D_3 \frac{\partial \varphi_y}{\partial y} + D_4 \frac{\partial^3 \varphi_y}{\partial y^3} = q(x, y) + \rho h \frac{\partial^2 w}{\partial t^2} - D_{11} \left( \frac{\partial^4 w}{\partial x^2 \partial t^2} + \frac{\partial^4 w}{\partial y^2 \partial t^2} \right) + D_{12} \left( \frac{\partial^3 \varphi_x}{\partial x \partial t^2} + \frac{\partial^3 \varphi_y}{\partial y \partial t^2} \right) \tag{20}$$

$$-D_4 \frac{\partial^3 w}{\partial x \partial y^2} + D_5 \frac{\partial^2 \varphi_y}{\partial y \partial x} + D_6 \frac{\partial^2 \varphi_x}{\partial y^2} + D_7 \frac{\partial^4 \varphi_y}{\partial x \partial y^3} - D_7 \frac{\partial^4 \varphi_x}{\partial y^4} + D_7 \frac{\partial^4 \varphi_y}{\partial y \partial x^3} - D_7 \frac{\partial^4 \varphi_x}{\partial y^2 \partial x^2} - D_3 \frac{\partial w}{\partial x} - D_3 \varphi_x - D_4 \frac{\partial^3 w}{\partial x^3} + D_8 \frac{\partial^2 \varphi_x}{\partial x^2} = -D_{12} \frac{\partial^3 w}{\partial x \partial t^2} + D_{13} \frac{\partial^2 \varphi_x}{\partial t^2} \tag{21}$$

$$-D_4 \frac{\partial^3 w}{\partial y \partial x^2} + D_9 \frac{\partial^2 \varphi_x}{\partial y \partial x} + D_{10} \frac{\partial^2 \varphi_y}{\partial x^2} + D_7 \frac{\partial^4 \varphi_y}{\partial x^4} + D_7 \frac{\partial^4 \varphi_y}{\partial x^2 \partial y^2} - D_7 \frac{\partial^4 \varphi_x}{\partial y \partial x^3} - D_7 \frac{\partial^4 \varphi_x}{\partial x \partial y^3} - D_4 \frac{\partial^3 w}{\partial y^3} - D_3 \frac{\partial w}{\partial y} - D_3 \varphi_y + D_8 \frac{\partial^2 \varphi_y}{\partial y^2} = -D_{12} \frac{\partial^3 w}{\partial y \partial t^2} + D_{13} \frac{\partial^2 \varphi_y}{\partial t^2} \tag{22}$$

### 7. Navier's solution method

The Navier's solution method is applicable to rectangular plates with simply-supported boundary conditions at all edges. Because the boundary conditions are spontaneously satisfied in this way, the functions of the plate's mid-plane are expressed as double trigonometric series [13 & 11]:

$$W(x, y, t) = \sum_{m=1}^{\infty} \sum_{n=1}^{\infty} W_{mn} \sin \alpha x \sin \beta y e^{i\omega t} \tag{23}$$

$$\varphi_x(x, y, t) = \sum_{m=1}^{\infty} \sum_{n=1}^{\infty} X_{mn} \cos \alpha x \sin \beta y e^{i\omega t} \tag{24}$$

$$\varphi_y(x, y, t) = \sum_{m=1}^{\infty} \sum_{n=1}^{\infty} Y_{mn} \sin \alpha x \cos \beta y e^{i\omega t} \tag{25}$$

The load can also be calculated from the following relation:

$$q = \sum_{m=1}^{\infty} \sum_{n=1}^{\infty} Q_{mn} \sin \alpha x \sin \beta y e^{i\omega t} \tag{26}$$

$$Q_{mn} = \frac{4}{ab} \int_0^a \int_0^b q(x, y) \sin \alpha x \sin \beta y dx dy \tag{27}$$

$$Q_{mn} = \begin{cases} q_0 & ; \text{For sinusoidal force} \\ \frac{16q_0}{m\pi^2} & ; \text{For uniform force} \\ \frac{4Q_0}{ab} & ; \text{For point force in the plane center} \end{cases} \quad (28)$$

Where in:

$$\alpha = \frac{\pi m}{a}, \quad \beta = \frac{\pi n}{b}, \quad i = \sqrt{-1} \quad (29)$$

Simply-supported boundary conditions were also satisfied by the Navier's method according to the following equations:

$$\begin{aligned} x = 0 \quad & \left\{ \begin{aligned} w(0, y) = w(a, y) = \sum \sum w_{mn} \sin \frac{m\pi}{a} x \sin \frac{n\pi}{b} y = 0 \\ \varphi_y(0, y) = \varphi_y(a, y) = \sum \sum y_{mn} \sin \frac{m\pi}{a} x \cos \frac{n\pi}{b} y = 0 \end{aligned} \right. \end{aligned} \quad (30)$$

$$\begin{aligned} y = 0 \quad & \left\{ \begin{aligned} w(x, 0) = w(x, b) = \sum \sum w_{mn} \sin \frac{m\pi}{a} x \sin \frac{n\pi}{b} y = 0 \\ \varphi_x(x, 0) = \varphi_x(x, b) = \sum \sum x_{mn} \cos \frac{m\pi}{a} x \sin \frac{n\pi}{b} y = 0 \end{aligned} \right. \end{aligned} \quad (31)$$

## 8. The matrix of equations

The general matrix of the third-order plate equations along with the auxiliary equations are obtained using the Navier's solution ( $R_1 - R_9$  &  $G_1 - G_9$  are given in the appendix)

$$\left( \begin{bmatrix} R_1 & R_2 & R_3 \\ R_4 & R_5 & R_6 \\ R_7 & R_8 & R_9 \end{bmatrix} - \omega^2 \begin{bmatrix} G_1 & G_2 & G_3 \\ G_4 & G_5 & G_6 \\ G_7 & G_8 & G_9 \end{bmatrix} \right) \begin{bmatrix} w_{mn} \\ X_{mn} \\ Y_{mn} \end{bmatrix} = \begin{bmatrix} Q_{mn} \\ 0 \\ 0 \end{bmatrix} \quad (32)$$

Various materials such as epoxy, graphene, copper and so on can be considered as the plate's material. In this study, graphene is chosen as the plate's material. A single-layer graphene plate has the following properties [12]:

$$E = 1.06 \text{TPa}, \nu = 0.25, h = 0.34 \text{nm}, \rho = 2250 \text{kg/m}^3$$

Also, the relationship between  $E$  and  $\mu$  and  $\nu$  can be written as following:

$$\lambda = \frac{\nu E}{(1 + \nu)(1 - 2\nu)}, \quad \mu = \frac{E}{2(1 + \nu)} \quad (33)$$

Where  $E$  is Young's modulus and  $\mu$  and  $\lambda$  are lame coefficients [14]. Also, the value of the force  $q = 1 \text{N/m}^2$  was considered.

## 9. Results and discussion

The computational program was written in Matlab software, and the results were obtained using this program. All boundary conditions were also considered as simply-supported.

Figure 2 shows the third-order nanoplate bending rate under uniform surface traction for the length to width ratio and length to thickness ratio. As shown in the figure, with increasing the length parameter to the thickness of the nanoplate, the bending ratio decreased. Furthermore, the bending ratio increased with increasing aspect ratio of the nanoplate.

Table 1 shows the dimensionless bending values of the third-order nanoplate under the sinusoidal load for the ratio of length to width and ratio of length to thickness. As shown in the table, with increasing length to the thickness parameter, the dimensionless bending value of the nanoplate decreased. Moreover, with increasing aspect ratio of the nanoplate, the dimensionless bending value increased except for the state that the length scale parameter was ignored.

Table 2 compares the dimensionless bending values of different nanoplates under the sinusoidal load for different length to width ratios. As can be seen in the table, the dimensionless bending value was the highest for Kirchhoff's nanoplate and the lowest for the Mindlin's nanoplate.

Figure 3 shows the frequency of third-order nanoplate different modes ( $\omega_{11}$ - $\omega_{12}$ - $\omega_{21}$ - $\omega_{22}$ ). This value decreased due to an increase in length parameter to thickness. Similarly, frequency was the lowest for the first mode and increased for the next modes.

Table 3 compares the third-order nanoplate different modes' frequencies for different length to width ratios. As can be seen, with increasing the aspect ratio, the vibration frequency value for different modes decreased.

Table 4 shows the frequency of different modes ( $\omega_{11}$ - $\omega_{12}$ - $\omega_{21}$ - $\omega_{22}$ ) for diverse nanoplates. According to the table, the frequency value was the highest for the Mindlin's nanoplate and the lowest for the third-order nanoplate.

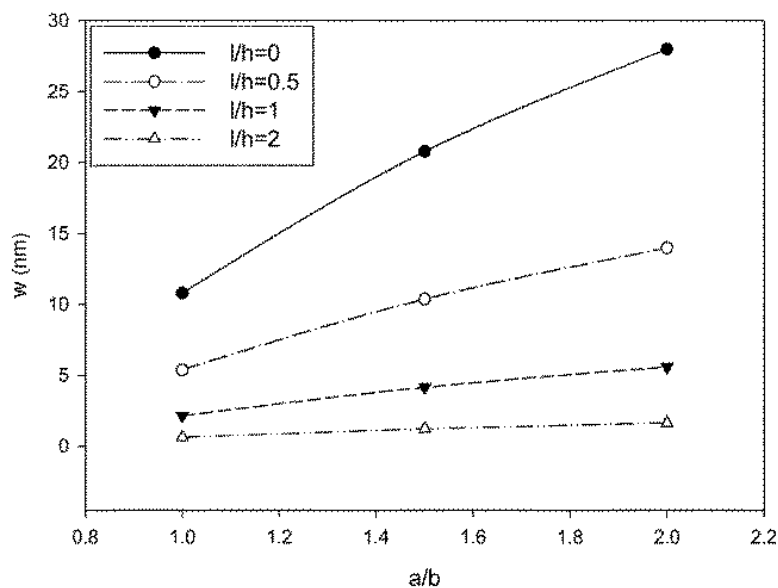


Figure 2. The third-order nanoplate bending rate under uniform surface traction for the length to width ratio and length to thickness ratio ( $q=1e-18$  N/nm<sup>2</sup>  $a/h=30$ )

Table 1. The dimensionless bending value of the third-order nanoplate under the sinusoidal load for length to width ratio and length to thickness ratio ( $q=1e-18$  N/nm<sup>2</sup>  $a/h=30$ )

a/b	l/h			
	0	0.5	1	2
1	1.00000	0.49858	0.19912	0.05852

1.5	1.00000	0.49883	0.19927	0.05858
2	1.00000	0.49895	0.19935	0.05860

**Table 2.** The dimensionless bending value comparison of the various nanoplate under the sinusoidal load effect for length to width ratio ( $q=1e-18$  N/nm<sup>2</sup>,  $l/h=1$   $a/h=30$ )

$a/b$	Kirchhoff plate	Mindlin plate	Third order shear deformation plate	$N$ order shear deformation plate ( $n=5$ )
1	0.2	0.072264	0.19912	0.19907
1.5	0.2	0.072121	0.19927	0.19923
2	0.2	0.072049	0.19935	0.19931

**Table 3.** The frequencies comparison of third-order nanoplate different modes for length to width ratio ( $a/h=30$ )

Mode	$l/h$			
	0	0.5	1	2
$a/b=1$				
$\omega_{11}$	13.9441	19.7447	31.2407	57.6223
$\omega_{12}$	34.6497	49.1546	77.8533	143.6613
$\omega_{21}$	34.6497	49.1546	77.8533	143.6613
$\omega_{22}$	55.1098	78.3225	124.1752	229.2384
$\omega_{33}$	121.6342	173.8911	276.5826	511.3107
$a/b=2$				
$\omega_{11}$	8.7284	12.3536	19.5411	36.0389
$\omega_{12}$	13.9441	19.7447	31.2407	57.6223
$\omega_{21}$	29.4967	41.8251	66.2277	122.1954
$\omega_{22}$	34.6497	49.1546	77.8533	143.6613
$\omega_{33}$	77.0069	109.6563	174.0385	321.4395

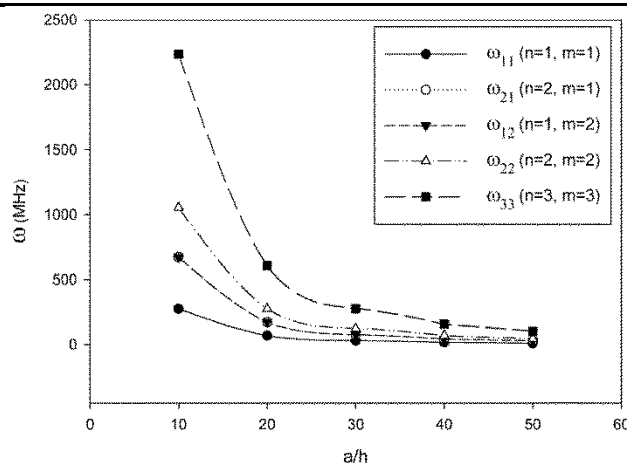


**Figure 3.** The frequencies comparison of third-order nanoplate different modes for length to width ratio ( $a/b=1$ ,  $l/h=1$ )

**Table 4.** The frequencies comparison of numerous nanoplate different modes for the various length to width ratios ( $l/h=1$ ,  $a/b=1.5$ )

Mode	$a/h$		
	20	30	40



Mindlin plate			
$\omega_{11}$	83.8680	37.5829	21.2022
$\omega_{12}$	159.1488	071.8354	40.6324
$\omega_{21}$	250.5691	114.0783	64.7336
$\omega_{22}$	321.6951	147.4292	83.8680
Kirchhoff plate			
$\omega_{11}$	50.8001	22.5964	12.7141
$\omega_{12}$	97.5592	43.4282	24.4419
$\omega_{21}$	155.8295	69.4324	39.0903
$\omega_{22}$	202.3037	90.2074	50.8001
Third order shear deformation plate			
$\omega_{11}$	50.6984	22.5761	12.7077
$\omega_{12}$	97.1889	43.3538	24.4182
$\omega_{21}$	154.8989	69.2435	39.0300
$\omega_{22}$	200.7540	89.8902	50.6984

## 10. Conclusion

In this study, the bending and vibration of third-order nanoplate were investigated using the modified couple stress theory. As observed in the tables and figures, the third-order nanoplate bending rate under uniform load effect, decreased with increasing the length to thickness ratio parameter of the nanoplate, however, the bending ratio increased with increasing aspect ratio. Also, the third-order nanoplate dimensionless bending value under the sinusoidal load, decreased with increasing length to thickness ratio parameter. Furthermore, the dimensionless bending value increased with increasing aspect ratio except for the state that the length scale parameter was ignored. The dimensionless bending value was also the highest for Kirchhoff's nanoplate and the lowest for Mindlin's nanoplate. In addition, the frequency of the third-order nanoplate different modes, decreased with increasing the length to thickness ratio. Additionally, the frequency value for the first mode was the lowest value and increased for the next modes. Moreover, different modes' vibration frequency was decreased by increasing aspect ratio.

## References

- [1] Daikh, A. A., Houari, M. S. A., & Eltaher, M. A. (2020). A novel nonlocal strain gradient Quasi-3D bending analysis of sigmoid functionally graded sandwich nanoplates. *Composite Structures, In Press*, 113347.
- [2] Yang, Y., Hu, Z.-L. and Li, X.-F. (2021). Axisymmetric bending and vibration of circular nanoplates with surface stresses. *Thin-Walled Structures*, 166, 108086.
- [3] Shafiei, Z., Sarrami-Foroushani, S., Azhari, F. and Azhari, M. (2020). Application of modified couple-stress theory to stability and free vibration analysis of single and multi-layered graphene sheets. *Aerospace Science and Technology*, 98, 105652.
- [4] Thanh, C.-L., Tran, L. V., Vu-Huu, T. and Abdel-Wahab, M. (2019). The size-dependent thermal bending and buckling analyses of composite laminate microplate based on new modified couple stress theory and isogeometric analysis. *Computer Methods in Applied Mechanics and Engineering*, 350, 337-361.
- [5] Yang, F., Chong, A.C.M., Lam, D.C.C., Tong, P. (2002). Couple stress Based Strain gradient theory for elasticity. *Int.J.Solids Struct*, 39, 2731-2743.
- [6] Toupin, R.A. (1962). Elastic materials with couple stresses. *Arch.Rational Mech.Anal*, 11, 385-414.

- [7] Mindlin, R.D., Tiersten, H.F. (1962). Effects of couple-stresses in linear elasticity. *Arch. Rational Mech. Anal*, 11, 415–448.
- [8] Koiter, W.T. (1964). Couple stresses in the theory of elasticity. *I and II. Proc .K. Ned. Akad .Wet.(B)* 67, 17–44.
- [9] Mindlin, R.D. (1964). Micro-structure in linear elasticity. *Arch. Rational Mech. Anal*, 16, 51–78.
- [10] Tsiatas, G.C. (2009). A new kirchhoff model based on a modified couple stress theory. *International Journal of solids and structures*, 46, 2757-2764.
- [11] Tai, T., Ho Choi, D. (2013). size-dependent functionally graded kirchhoff and mindlin plate theory based on a modified couple stress theory. *Composite Structures*, 95, 142-153.
- [12] B. Akgoz, Civalek. O. (2012). Free vibration analysis for single –layered graphene sheets in an elastic matrix via modified couple stress theory. *Materials and Design*, 42, 164-171.
- [13] Wang, B., Zhou, S., Zhao, J., Chen, X. (2011). A size-dependent kirchhoff micro-plate model based on strain gradient elasticity theory. *European Journal of mechanics A/Solids*, 30, 517-524.
- [14] Roque, C.M.C., Ferreira, A.J.M., Reddy, J.N. (2013). Analysis of mindlin micro plates with a modified couple stress theory and meshless method. *Applied Mathematical Modeling*, 37, 4626-4633.

## APPENDIX:

strain tensors:

$$\varepsilon_{xx} = z \frac{\partial \varphi_x}{\partial x} - \frac{4}{3} \left(\frac{1}{h}\right)^2 z^3 \left(\frac{\partial^2 w}{\partial x^2} + \frac{\partial \varphi_x}{\partial x}\right) \quad (1)$$

$$\varepsilon_{yy} = z \frac{\partial \varphi_y}{\partial y} - \frac{4}{3} \left(\frac{1}{h}\right)^2 z^3 \left(\frac{\partial^2 w}{\partial y^2} + \frac{\partial \varphi_y}{\partial y}\right) \quad (2)$$

$$\varepsilon_{zz} = 0 \quad (3)$$

$$\varepsilon_{xy} = \varepsilon_{yx} = \frac{1}{2} z \left(\frac{\partial \varphi_x}{\partial y} + \frac{\partial \varphi_y}{\partial x}\right) - \frac{2}{3} \left(\frac{1}{h}\right)^2 z^3 \left(\frac{\partial \varphi_x}{\partial y} + \frac{\partial \varphi_y}{\partial x} + 2 \frac{\partial^2 w}{\partial x \partial y}\right) \quad (4)$$

$$\varepsilon_{xz} = \varepsilon_{zx} = \left(\frac{1}{2} - 2 \left(\frac{z}{h}\right)^2\right) \left(\frac{\partial w}{\partial x} + \varphi_x\right) \quad (5)$$

$$\varepsilon_{yz} = \varepsilon_{zy} = \left(\frac{1}{2} - 2 \left(\frac{z}{h}\right)^2\right) \left(\frac{\partial w}{\partial y} + \varphi_y\right) \quad (6)$$

symmetric part of the rotational vector: (7)

$$\theta_x = \frac{\partial w}{\partial y} - \left(\frac{1}{2} - 2 \left(\frac{z}{h}\right)^2\right) \left(\frac{\partial w}{\partial y} + \varphi_y\right)$$

$$\theta_y = -\frac{\partial w}{\partial x} + \left(\frac{1}{2} - 2 \left(\frac{z}{h}\right)^2\right) \left(\frac{\partial w}{\partial x} + \varphi_x\right) \quad (8)$$

$$\theta_z = \frac{1}{2} \left(z - \frac{4}{3} \left(\frac{1}{h}\right)^2 z^3\right) \left(\frac{\partial \varphi_y}{\partial x} - \frac{\partial \varphi_x}{\partial y}\right) \quad (9)$$

symmetric part of the curvature tensor: (10)

$$x_{xx} = \frac{\partial^2 w}{\partial x \partial y} - \left(\frac{1}{2} - 2\left(\frac{z}{h}\right)^2\right) \left(\frac{\partial^2 w}{\partial x \partial y} + \frac{\partial \varphi_y}{\partial x}\right)$$

$$x_{yy} = -\frac{\partial^2 w}{\partial x \partial y} + \left(\frac{1}{2} - 2\left(\frac{z}{h}\right)^2\right) \left(\frac{\partial \varphi_x}{\partial y} + \frac{\partial^2 w}{\partial x \partial y}\right) \tag{11}$$

$$x_{zz} = \left(\frac{1}{2} - 2\left(\frac{z}{h}\right)^2\right) \left(\frac{\partial \varphi_y}{\partial x} - \frac{\partial \varphi_x}{\partial y}\right) \tag{12}$$

$$x_{xy} = \frac{1}{2} \left(\frac{\partial^2 w}{\partial y^2} - \frac{\partial^2 w}{\partial x^2}\right) + \left(\frac{1}{4} - \left(\frac{z}{h}\right)^2\right) \left(\frac{\partial^2 w}{\partial x^2} + \frac{\partial \varphi_x}{\partial x} - \frac{\partial^2 w}{\partial y^2} - \frac{\partial \varphi_y}{\partial y}\right) \tag{13}$$

$$x_{xz} = \frac{1}{4} \left(z - \frac{4}{3} \left(\frac{1}{h}\right)^2 z^3\right) \left(\frac{\partial^2 \varphi_y}{\partial x^2} - \frac{\partial^2 \varphi_x}{\partial y \partial x}\right) + 2z \left(\frac{1}{h}\right)^2 \left(\frac{\partial w}{\partial y} + \varphi_y\right) \tag{14}$$

$$x_{yz} = -2z \left(\frac{1}{h}\right)^2 \left(\frac{\partial w}{\partial x} + \varphi_x\right) + \frac{1}{4} \left(z - \frac{4}{3} \left(\frac{1}{h}\right)^2 z^3\right) \left(\frac{\partial^2 \varphi_y}{\partial x \partial y} - \frac{\partial^2 \varphi_x}{\partial y^2}\right) \tag{15}$$

stress tensors: (16)

$$\sigma_{xx} = (\lambda + 2\mu)\epsilon_{xx} + \lambda\epsilon_{yy}$$

$$\sigma_{yy} = \lambda\epsilon_{xx} + (\lambda + 2\mu)\epsilon_{yy} \tag{17}$$

$$\sigma_{zz} = \lambda(\epsilon_{xx} + \epsilon_{yy}) \tag{18}$$

$$\sigma_{yx} = \sigma_{xy} = 2\mu \epsilon_{xy} \tag{19}$$

$$\sigma_{xz} = \sigma_{zx} = 2\mu \epsilon_{xz} \tag{20}$$

$$\sigma_{yz} = \sigma_{zy} = 2\mu \epsilon_{yz} \tag{21}$$

The coefficients of E: (22)

$$E_1 = \frac{\partial^2 w}{\partial x^2} [(\lambda + 2\mu)(C_3 - C_1 C_2) + \frac{1}{2}\mu l^2(1 + C_4) - \frac{1}{4}\mu l^2(1 + C_4)(1 - C_4)] + \frac{\partial^2 w}{\partial y^2} [\lambda(C_3 - C_1 C_2) - \frac{1}{2}\mu l^2(1 + C_4) + \frac{1}{4}\mu l^2(1 - C_4)(1 + C_4)] + \frac{\partial \varphi_x}{\partial x} [-(\lambda + 2\mu)(C_2 C_1) - \frac{1}{4}\mu l^2(1 - C_4)(1 + C_4)] + \frac{\partial \varphi_y}{\partial y} [-\lambda(C_2 C_1) - \frac{1}{4}\mu l^2(1 - C_4)(1 + C_4)]$$

$$E_2 = \frac{\partial^2 w}{\partial y^2} [(\lambda + 2\mu)(C_3 - C_1 C_2) + \frac{1}{2}\mu l^2(1 + C_4) - \frac{1}{4}\mu l^2(1 + C_4)(1 - C_4)] + \frac{\partial^2 w}{\partial x^2} [\lambda(C_3 - C_1 C_2) - \frac{1}{2}\mu l^2(1 + C_4) + \frac{1}{4}\mu l^2(1 - C_4)(1 + C_4)] + \frac{\partial \varphi_y}{\partial y} [-(\lambda + 2\mu)(C_2 C_1) - \frac{1}{4}\mu l^2(1 - C_4)(1 + C_4)] + \frac{\partial \varphi_x}{\partial x} [-\lambda(C_2 C_1) - \frac{1}{4}\mu l^2(1 - C_4)(1 + C_4)] \tag{23}$$

$$E_3 = \frac{\partial^2 w}{\partial x \partial y} [4\mu C_2^2 + \mu l^2(1 + C_4)^2] + \frac{\partial \varphi_x}{\partial y} [-2\mu C_2 C_1 - \frac{1}{2}\mu l^2(1 - C_4)(1 + C_4)] + \frac{\partial \varphi_y}{\partial x} [-2\mu C_2 C_1 - \frac{1}{2}\mu l^2(1 - C_4)(1 + C_4)] \tag{24}$$

$$E_4 = \left(\frac{\partial w}{\partial x} + \varphi_x\right) [\mu(1 - C_4)^2 + \frac{1}{4}\mu l^2 C_5^2] + \left(\frac{\partial^2 \varphi_y}{\partial x \partial y} - \frac{\partial^2 \varphi_x}{\partial y^2}\right) \left[\frac{1}{4}\mu l^2 C_5 C_1\right] \tag{25}$$

$$E_5 = \left(\frac{\partial w}{\partial y} + \varphi_y\right) [\mu(1 - C_4)^2 + \frac{1}{4}\mu l^2 C_5^2] + \left(\frac{\partial^2 \varphi_x}{\partial x \partial y} - \frac{\partial^2 \varphi_y}{\partial x^2}\right) \left[\frac{1}{4}\mu l^2 C_5 C_1\right] \tag{26}$$

$$E_6 = E_8 = \left(\frac{\partial w}{\partial x} + \varphi_x\right) \left[\frac{1}{4}\mu l^2 C_5 C_1\right] + \left(\frac{\partial^2 \varphi_y}{\partial x \partial y} - \frac{\partial^2 \varphi_x}{\partial y^2}\right) \left[\frac{1}{4}\mu l^2 C_1^2\right] \tag{27}$$

$$E_7 = E_9 = \left(\frac{\partial w}{\partial y} + \varphi_y\right) \left[-\frac{1}{4}\mu l^2 C_5 C_1\right] + \left(\frac{\partial^2 \varphi_y}{\partial x^2} - \frac{\partial^2 \varphi_x}{\partial x \partial y}\right) \left[\frac{1}{4}\mu l^2 C_1^2\right] \quad (28)$$

$$E_{10} = \frac{\partial^2 w}{\partial x^2} \left[ (\lambda + 2\mu)(C_1^2 - zC_1) - \frac{1}{4}\mu l^2(1 - C_4)(1 + C_4) \right] + \frac{\partial^2 w}{\partial y^2} \left[ \lambda C_1(-z + C_1) + \frac{1}{4}\mu l^2(1 - C_4)(1 + C_4) \right] + \frac{\partial \varphi_x}{\partial x} \left[ (\lambda + 2\mu)C_1^2 + \frac{1}{4}\mu l^2(1 - C_4)^2 \right] + \frac{\partial \varphi_y}{\partial y} \left[ \lambda C_1^2 - \frac{1}{4}\mu l^2(1 - C_4)^2 \right] \quad (29)$$

$$E_{11} = \frac{\partial^2 w}{\partial y^2} \left[ (\lambda + 2\mu)(C_1^2 - zC_1) - \frac{1}{4}\mu l^2(1 - C_4)(1 + C_4) \right] + \frac{\partial^2 w}{\partial x^2} \left[ \lambda A_1(-z + C_1) + \frac{1}{4}\mu l^2(1 - C_4)(1 + C_4) \right] + \frac{\partial \varphi_y}{\partial y} \left[ (\lambda + 2\mu)C_1^2 + \frac{1}{4}\mu l^2(1 - C_4)^2 \right] + \frac{\partial \varphi_x}{\partial x} \left[ \lambda C_1^2 - \frac{1}{4}\mu l^2(1 - C_4)^2 \right] \quad (30)$$

$$E_{12} = \frac{\partial^2 w}{\partial x \partial y} \left[ -2\mu C_2 C_1 - \frac{1}{2}\mu l^2(1 - C_4)(1 + C_4) \right] + \frac{\partial \varphi_x}{\partial y} \left[ \mu C_1^2 + \mu l^2(1 - C_4)^2 \right] + \frac{\partial \varphi_y}{\partial x} \left[ \mu C_1^2 - \frac{1}{2}\mu l^2(1 - C_4)^2 \right] \quad (31)$$

$$E_{13} = \frac{\partial^2 w}{\partial x \partial y} \left[ -2\mu C_2 C_1 - \frac{1}{2}\mu l^2(1 - C_4)(1 + C_4) \right] + \frac{\partial \varphi_x}{\partial y} \left[ \mu C_1^2 - \frac{1}{2}\mu l^2(1 - C_4)^2 \right] + \frac{\partial \varphi_y}{\partial x} \left[ \mu C_1^2 + \mu l^2(1 - C_4)^2 \right] \quad (32)$$

$$E_{14} = \left(\frac{\partial w}{\partial x} + \varphi_x\right) \left[ \mu(1 - C_4)^2 + \frac{1}{4}\mu l^2 C_5^2 \right] + \left(\frac{\partial^2 \varphi_y}{\partial x \partial y} - \frac{\partial^2 \varphi_x}{\partial y^2}\right) \left[ \frac{1}{4}\mu l^2 C_5 C_1 \right] \quad (33)$$

$$E_{15} = \left(\frac{\partial w}{\partial y} + \varphi_y\right) \left[ \mu(1 - C_4)^2 + \frac{1}{4}\mu l^2 C_5^2 \right] + \left(\frac{\partial^2 \varphi_x}{\partial x \partial y} - \frac{\partial^2 \varphi_y}{\partial x^2}\right) \left[ \frac{1}{4}\mu l^2 C_5 C_1 \right] \quad (34)$$

The coefficients of C: (35)

$$C_1 = z - \frac{4}{3} \left(\frac{1}{h}\right)^2 z^3$$

$$C_2 = \frac{4}{3} \left(\frac{1}{h}\right)^2 z^3 \quad (36)$$

$$C_3 = \frac{4}{3} \left(\frac{1}{h}\right)^2 z^4 \quad (37)$$

$$C_4 = 4 \left(\frac{z}{h}\right)^2 \quad (38)$$

$$C_5 = -8z \left(\frac{1}{h}\right)^2 \quad (39)$$

$$C_6 = \frac{4}{3} \left(\frac{1}{h}\right)^2 \quad (40)$$

$$C_7 = \mu \frac{h}{3} \quad (41)$$

$$C_8 = \mu \frac{h}{5} \quad (42)$$

$$C_9 = \frac{h^3}{252} (\lambda + 2\mu) \quad (43)$$

$$C_{10} = (\lambda + 2\mu) \frac{h^3}{60} \quad (44)$$

$$C_{11} = \mu l^2 \frac{4}{3h} \quad (45)$$

$$C_{12} = \frac{1}{4}\mu l^2 h \quad (46)$$

The coefficients of D: (47)

$$D_1 = 2C_{12} + l^2 C_7 + \frac{1}{2}l^2 C_8 + 2C_9 \quad (48)$$

$$D_2 = \frac{1}{2}D_1 = C_{12} + C_9 + \frac{1}{2}l^2 C_7 + \frac{1}{4}l^2 C_8 \quad (49)$$

$$D_3 = -\mu h + 2C_7 - C_8 - C_{11} \quad (50)$$

$$D_4 = C_9 - C_{10} + \frac{1}{4}l^2 C_8 - C_{12} \quad (51)$$

$$D_5 = 3C_{12} - \frac{3}{2}l^2 C_7 + \frac{3}{4}l^2 C_8 - (\lambda + \mu)I_2 + 2(\lambda + \mu)C_6 I_4 - (\lambda + \mu)C_6^2 I_6 \quad (52)$$

$$D_6 = -\mu I_2 + 2\mu C_6 I_4 - \mu C_6^2 I_6 - 4C_{12} + 2l^2 C_7 - l^2 C_8 \quad (53)$$

$$D_7 = \frac{1}{4}\mu l^2 I_2 - \frac{1}{2}\mu l^2 C_6 I_4 + \frac{1}{4}\mu l^2 C_6^2 I_6 \quad (54)$$

$$D_8 = -(\lambda + 2\mu)I_2 + 2C_{10} - C_9 - C_{12} + \frac{1}{2}l^2 C_7 - \frac{1}{4}l^2 C_8 \quad (55)$$

$$D_9 = \frac{5}{4}l^2 C_8 - \frac{3}{2}\mu l^2 C_6^2 I_4 - \frac{5}{2}l^2 C_7 + 3C_{12} - (\lambda + \mu)I_2 - (\lambda + \mu)C_6^2 I_6 + 2(\lambda + \mu)C_6 I_4 \quad (56)$$

$$D_{10} = 3l^2 C_7 - \frac{3}{2}l^2 C_8 + \frac{3}{2}\mu l^2 C_6^2 I_4 - \mu I_2 - \mu C_6^2 I_6 + 2\mu C_6 I_4 - 4C_{12} \quad (57)$$

$$D_{11} = \rho C_6^2 I_6 \quad (58)$$

$$D_{12} = \rho C_6 I_4 - \rho C_6^2 I_6 \quad (59)$$

$$D_{13} = \rho I_2 - 2\rho C_6 I_4 - \rho C_6^2 I_6 \quad (59)$$

The coefficients of R: (60)

$$R_1 = D_1 \alpha^2 \beta^2 + D_2 \alpha^4 + D_2 \beta^4 - D_3 \alpha^2 - D_3 \beta^2$$

$$R_2 = R_4 = D_4 \alpha^3 + D_4 \alpha \beta^2 - D_3 \alpha \quad (61)$$

$$R_3 = R_7 = D_4 \beta^3 + D_4 \alpha^2 \beta - D_3 \beta \quad (62)$$

$$R_5 = -D_7 \beta^4 - D_7 \alpha^2 \beta^2 - D_6 \beta^2 - D_8 \alpha^2 - D_3 \quad (63)$$

$$R_6 = D_7 \alpha \beta^3 + D_7 \alpha^3 \beta - D_5 \alpha \beta \quad (64)$$

$$R_8 = -D_7 \alpha^3 \beta - D_7 \alpha \beta^3 - D_9 \alpha \beta \quad (65)$$

$$R_9 = D_7 \alpha^4 + D_7 \alpha^2 \beta^2 - D_{10} \alpha^2 - D_8 \beta^2 - D_3 \quad (66)$$

The coefficients of G:

$$G_1 = -D_{11} \alpha^2 - D_{11} \beta^2 - \rho h$$

$$G_2 = G_4 = D_{12}\alpha \quad (67)$$

$$G_3 = G_7 = D_{12}\beta \quad (68)$$

$$G_5 = G_9 = -D_{13} \quad (69)$$

$$G_6 = G_8 = 0 \quad (70)$$

$$G_6 = G_8 = 0 \quad (71)$$